Original article

Redox condition and organic carbon accumulation mechanism in the Cryogenian Nanhua Basin, South China: Insights from iron chemistry and sulfur, carbon, oxygen isotopes of the Datangpo Formation

Chaoyong Wang[1], Guanzhong Shi[2] *

[1]*Key Laboratory of CBM Resource and Reservoir-generating Process of Ministry of Education,*
China University of Mining and Technology, Xuzhou 221008, P. R. China
[2]*Key Laboratory of Tectonics and Petroleum Resources, Ministry of Education,*
China University of Geosciences, Wuhan 430074, P. R. China

Abstract:
Global glaciation, oxidation event and eukaryotic expansion and diversification in the Neoproterozoic period are marked events that characterize the early evolution of the Earth, but how the interactions occurred among these events is not well understood. The organic matters preserved in the black shales of the Datangpo Formation (Cryogenian period) are sensitive to redox conditions, and thus its accumulation and preservation offer beneficial clues to unravel the early evolutional history of the Earth. This study presents new chemostratigraphic data of iron component, total organic carbon content, sulfur isotope of pyrite, carbon and oxygen isotopes of carbonaceous shale of the Datangpo Formation (Cryogenian period) in the Datangpo section, South China. The analyzed results imply abundant nutrients existing in the ocean in the Early Cryogenian. The nutrients, such as phosphorus, resulting from neighbor volcanic eruptions, provided nutrients that enabled microbes to flourish during the Cryogenian interglacial gap. Iron components and sulfur isotopes indicated anoxic, euxinic deep water environments for the black shales in the lower portion of the Datangpo Formation. The anoxic setting was good for the preservation of organic matter, but terrigenous materials inputs, as revealed by the high Al_2O_3 contents, diluted the total organic carbon content.

1. Introduction

Organic-rich rocks are the research subject of great interest for several decades (Lazar et al., 2015; Ilgen et al., 2017; Jiang et al., 2017; Liu et al., 2017), because these rocks are the primary source of hydrocarbon resource (Johnson et al., 2016), and also because organic-rich rocks bear critical clues for the interaction between Earth surface environments and the biosphere in geological histories (Dodd et al., 2017; Yeasmin et al., 2017). Several factors can influence the origin of organic-rich rocks, including productivity, preservation, dilution, and any combinations of these factors (He et al., 2017). Productivity and preservation of organic matter are greatly influenced by the paleoenvironment and relevant redox condition (Arthur and Sageman, 1994).

The paleoenvironment of Cryogenian period (720 to 635 million years ago) is important for us to understand the evolution of early life on Earth (Scott et al., 2008; Planavsky et al., 2010). A series of marked geological events occurred in this stage, such as the break-up and assembly of Rodinian supercontinent, global glaciation, the second Great Oxidation Event and eukaryotic expansion (Zhu et al., 2007). These events greatly reshaped the paleogeography and paleoenvironment of the Earth surface, which is well preserved in sedimentary rocks (Shi et al., 2016, 2018; Wei et al., 2017).

The Neoproterozoic Nanhua Basin was a rift basin in the Yangtze Block caused by the breakup of the Rodinian supercontinent (Wang and Li, 2003). It has accommodated thick sediments, of which the Datangpo Formation was deposited
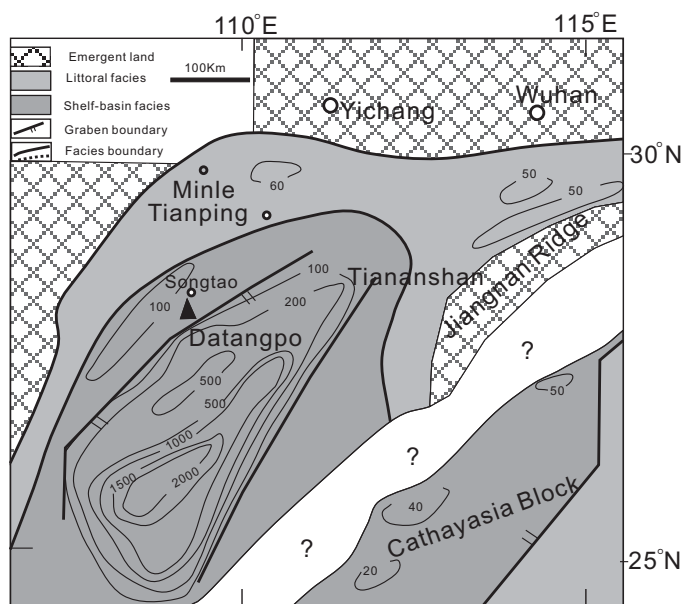
Fig. 1. Sedimentary lithofacies, paleogeographic and paleobathymetric map of the Nanhua Basin during glacial deposition of the Nantuo Formation (after Li et al., 2012).

in an interglacial period. A great deal of research has been conducted on the geochemical characteristics of the strata to unravel the paleoenvironment and their linkage with Great Oxidation Event and early life explosion (Li et al., 2017). For example, the analysis of iron and molybdenum elements, sulfur and nitrogen isotopes indicated a stratified redox marine environment (Li et al., 2012; Wei et al., 2017). However, the organic matter accumulation mechanism and its relationship with the stratified redox waters are ambiguous. The Datangpo Formation has a thick interval of black shale rocks that are rich in organic materials, and thus provide an excellent target to refine paleoenvironment and organic matter accumulation.

In this paper, we chose the Datangpo Formation from the Datangpo section in the Guizhou province to conduct iron component and total organic carbon (TOC) chemical analysis, and sulfur, carbon, oxygen isotopic measurement. Two main questions are addressed here: First, the organic carbon accumulation mechanism in an interglacial stage of the Cryogenian period; second, the coupling relationship between biological flourishing and paleoenvironment.

2. Geological setting

The Neoproterozoic Nanhua Basin is located in the southern margin of the Yangtze Block, occupied some portions of the Hunan province and the Guizhou province. It developed as a rift basin resulting from breakup of the Rodinian supercontinent at ~820 Ma (Wang and Li, 2003). Three sedimentary formations have been recognized in the Cryogenian strata, from base to top namely: Gucheng Formation, Datangpo Formation and Nantuo Formation (Li et al., 2012). The Gucheng and Nantuo formations are characterized by glacial diamictite of the Sturtian and Marinoan ice ages, respectively (Macdonald et al., 2010), while the between Datangpo Formation represents the interglacial succession composed of manganese-bearing

carbonate, black shale, and siltstone. The timing of the interglacial interval is suggested by zircon U-Pb ages of 663 ± 4 Ma and 654.5 ± 3.8 Ma (Zhou et al., 2004; Zhang et al., 2008) which were obtained in the tuffaceous beds at the basal and top of the formation, respectively. The overlying Ediacaran Doushantuo Formation is composed of post-glacial marine shales and carbonates containing multicellular fossil algae and achritarchs, some of which might represent the Earth's earliest animal embryos (Yin et al., 2007; Cohen et al., 2009).

The thickness of the Cryogenian deposits is various in different locations, with a total thickness of $> 2,000$ m in the basinal facies in the southeast and about 100 m in the shelf facies in the northwest (Wang and Li, 2003). Based on the distribution of glacial deposits of the Nantuo Formation, a confined marginal basin was suggested, with the range of deep waters distributing along a northwest-to-southeast axis, barely connection with the open ocean (Fig. 1; Wang and Li, 2003).

The samples were collected from the Datangpo section (Songtao Town) in the Guizhou province, where the Datangpo Formation was divided into two members. The lower member consists of black carbonaceous shales with manganese, with thickness of 13.4 m. The upper member consists of gray silty shale with thickness of 437 m. This study collects 20 black shales and 2 manganese ore samples in this section (Table 1).

3. Methods

The fresh samples are cleaned with distilled water 3 times to remove surface impurities, and then dry the samples in 105 °C for 6 hours in drying box, and finally take the samples in sealed capsules for testing. Microscopic observation uses Quanta 250 scanning electron microscope produced by American FEI Company.

Major and trace elements were completed in the modern

Table 1. Selected geochemical elements, iron compositions and sulfur isotopes in the shales of the Datangpo Formation in the Datangpo section.

Strata	Petrology	Sample NO.	Thickness (m)	TOC (%)	SiO$_2$ (%)	Al$_2$O$_3$ (%)	S (%)	P (%)	Mn (%)	δ^{34}S (‰)	Fe^T (%)	Fe$_{PY}$ (%)	Fe$_{HR}$ (%)	Fe$_{HR}$/Fe^T	Fe$_{PY}$/Fe$_{HR}$
Upper member	Silt shale	D26	95.0	0.35	65.11	20.32	0.61	0.02	0.00	-	1.68	0.07	0.44	0.26	0.15
		D25	40.0	0.50	62.51	20.61	0.09	0.03	0.00	-	1.49	0.18	0.43	0.29	0.41
		D24	13.0	1.06	58.95	19.13	0.18	0.04	0.31	-	0.27	0.04	0.07	0.25	0.65
	Shale	D15	0.4	5.58	66.42	17.71	1.07	0.11	1.13	-	0.54	0.08	0.13	0.23	0.66
		D14	0.1	13.53	20.21	7.72	0.11	0.17	25.71	58.91	0.82	0.64	0.69	0.84	0.93
	Carbonaceous shale	D13	0.7	8.14	65.72	18.71	0.12	0.04	0.04	61.16	2.41	1.75	2.21	0.92	0.79
		D12	0.1	5.67	58.63	16.26	0.84	0.03	0.44	-	4.38	1.86	2.22	0.51	0.84
		D11	1.5	4.78	69.71	16.21	1.41	0.03	0.21	-	3.74	2.27	2.58	0.69	0.88
		D10	1.4	5.65	49.52	18.12	2.48	0.31	0.30	-	3.01	2.00	2.54	0.84	0.79
	Shale	D9	0.2	0.51	49.52	31.62	0.41	0.07	0.06	-	0.42	0.25	0.36	0.86	0.69
Lower member	Carbonaceous shale	D8	0.1	7.56	58.13	18.81	2.71	0.01	0.11	61.50	1.39	0.96	1.17	0.84	0.82
		D7	1.3	6.16	60.71	17.32	1.42	0.11	0.40	60.53	2.91	1.78	2.53	0.87	0.70
		D6	0.1	6.19	55.60	16.31	0.81	0.03	0.05	-	2.89	1.82	2.40	0.83	0.76
	Shale	D5	1.1	2.19	58.41	15.91	2.58	0.03	2.81	58.67	3.14	2.15	2.43	0.77	0.88
		D4	0.1	7.15	54.92	20.01	2.43	0.04	0.02	-	3.61	2.84	3.42	0.95	0.83
	Carbonaceous shale	D3	1.2	6.78	56.74	20.21	2.19	0.02	0.03	53.56	2.58	3.20	2.66	0.83	0.87
		D2	1.7	6.19	64.91	16.11	1.62	0.50	0.04	52.55	2.98	2.91	2.54	0.85	0.82
	Ore	MN-2	1.5	-	-	-	-	-	-	62.85	2.13	0.09	1.30	0.61	0.50
		MN-1	1.6	-	-	-	-	-	-	60.50	2.72	0.32	1.24	0.46	0.07
	Shale	D1-3	0.7	3.68	66.21	15.72	0.51	0.02	2.20	-	1.82	0.60	1.19	0.66	0.07
		D1-2	0.15	1.23	61.12	21.87	0.11	0.11	0.71	61.22	0.46	0.12	0.40	0.87	0.31
		D1-1	0.15	0.85	66.91	19.51	0.04	0.03	0.05	-	1.12	0.22	0.95	0.85	0.23

Fe contents lower than 0.5% are invalid and would not be considered in this study.-. no measurement.
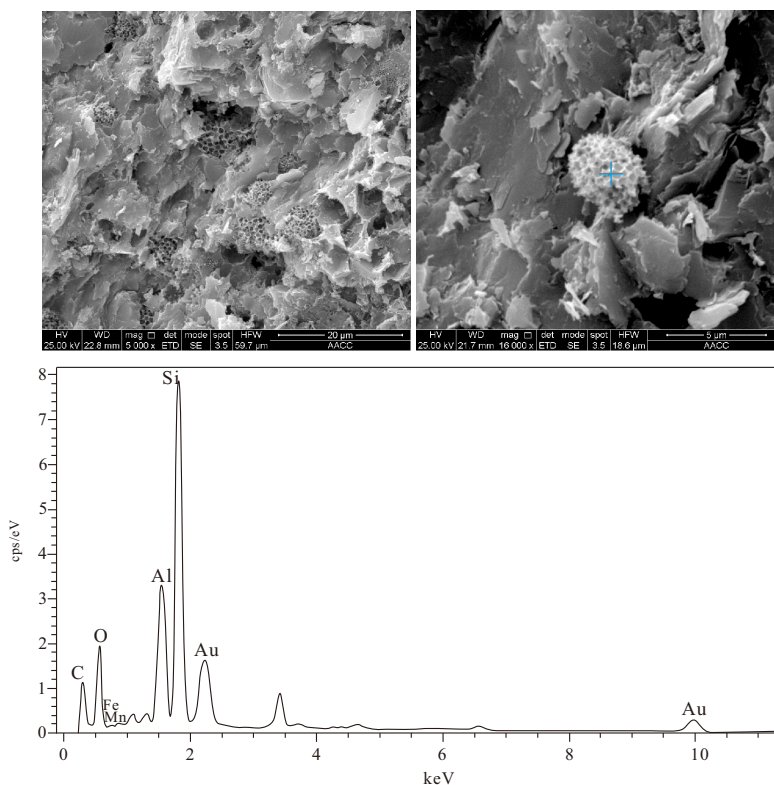
Fig. 2. Test of morphology and energy dispersive spectrometer (EDS) analysis of cyanobacterial cells.

analysis and testing center of China University of Mining and Technology. Major elements use X ray fluorescence spectrometer produced by Germany Brook AXS company (BRUKER S8 TIGER) and the test precision is < 8%. The chemical measurement of pyrite was converted on the basis of the sulfur content of pyrite. Iron oxides/hydroxides, carbonates and magnetite were measured by a continuous extraction method according to (Poulton and Canfield, 2005).

Iron composition was measured by chromium reduction method (Canfield et al., 1986) in the State Key Laboratory of biological geology and environmental geology, China University of Geosciences (Wuhan). Carbon and oxygen isotopes were tested in the State Key Laboratory of biological geology and environmental geology and the modern analysis and testing center of China University of Mining and Technology. Sulfur isotope of pyrite was analyzed by a Quadrupole Inductively coupled plasma mass spectrometer (ICP-MS). Organic carbon content was tested by combustion method, which was completed by the Jiangsu Institute of geological and mineral design.

4. Results

The test results of the major elements, trace elements, iron components, and sulfur isotopes of pyrite are shown in Table 1.

4.1 Organic matter content and phosphorus content

The carbonaceous shales of the lower member of the Datangpo Formation are rich in organic matters. TOC is between 0.51% and 13.53%, and most samples (more than 90% samples) show that the proportions of organic carbon content are commonly more than 5% with an average content of 6.3%, implying that the shales are of high-quality hydrocarbon source rocks.

The organic matter is mainly amorphous I type kerogen, and the original organism is mainly algae. The scanning morphology of cyanobacterial cells suggest they have been metasomatized into ferrous carbonate and gold-bearing silicate complexes while keeping the original cell textures (Fig. 2), and the elemental contents are listed in Table 2.

The phosphorus content is 0.021%-0.145% in the lower member of the Datangpo Formation, and the phosphorus content is 0.012%-0.013% in the upper member. Although a regularly positive correlation wasn't shown between the content of organic carbon and the content of phosphorus, samples of high phosphorus content generally contain high amount of organic carbon (Fig. 3(a)).

4.2 Fe chemistry, sulfur isotope and redox condition

The total Fe (Fe^T) ranges from 0.27% to 4.38%. Fe is essential elements for the microorganism growth, but there is no obvious linear correlation between the TOC and total Fe
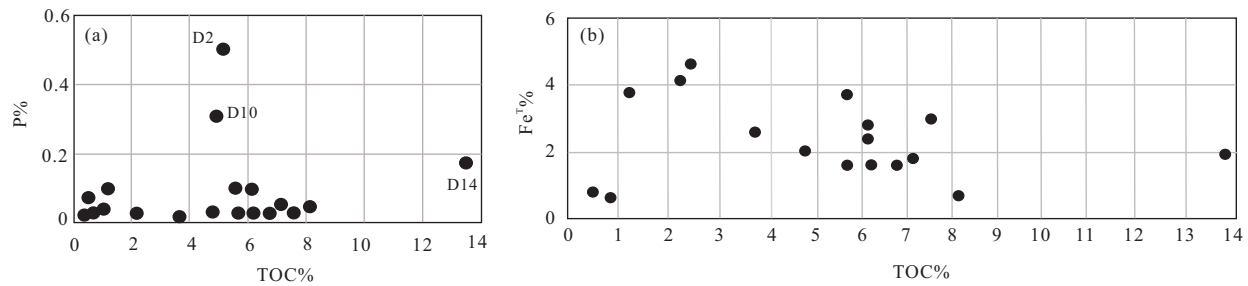
Fig. 3. Relationship of the phosphorus, total iron composition and TOC. (a) Relationship between phosphorus and TOC; (b) relationship between iron and TOC, and it shows a slightly negative relationship when TOC is more than 2%.
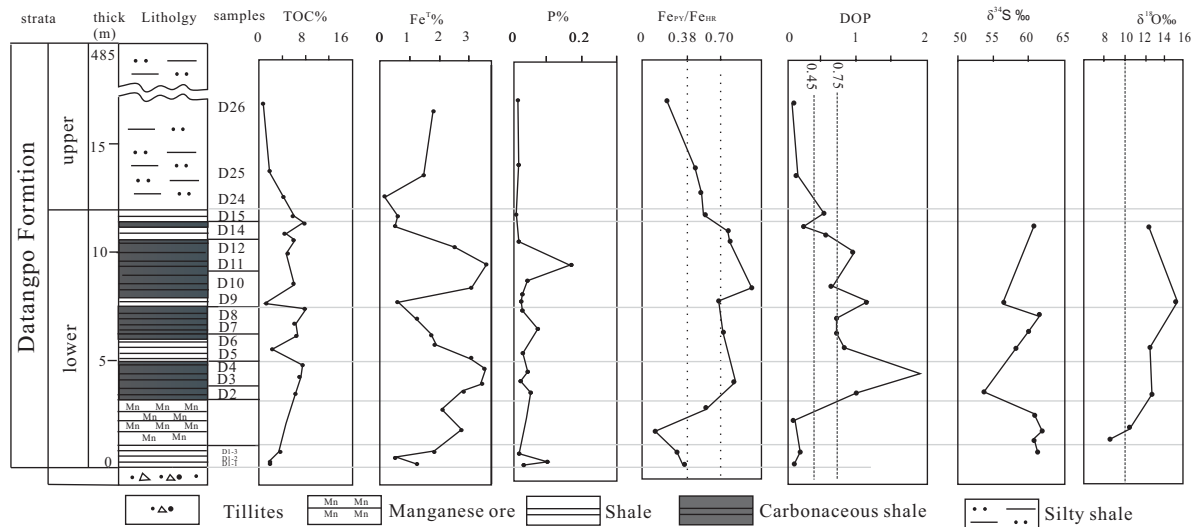
Fig. 4. The lithology and analyzed chemical data in the Datangpo Formation.

Table 2. Chemical composition of cyanobacterial cells by energy dispersive spectrometer (EDS) analysis.

Element	Weight (%)	Atomic (%)	Error (1σ) (%)
C	32.80	50.10	5.11
O	31.07	35.64	4.27
Si	12.99	8.49	0.46
Al	5.96	4.05	0.26
Mn	0.16	0.05	0.05
Fe	0.36	0.12	0.05
Au	16.67	1.55	0.54
Total	100.00	100.00	-

(Fe^T) (Fig. 3(b)).

To estimate redox condition in the Cryogenian period, we examined the concentrations of total Fe (Fe^T), pyrite iron (Fe_{py}), and highly reactive iron (Fe_{HR}) in the sedimentary rocks of the Datangpo Formation. The reactive iron (Fe_{HR}) was defined as $Fe_{HR} = Fe_{py}$ + ferric oxides (Fe_{ox}) + Fe magnetite (Fe_{mag}) + Fe carbonates (Fe_{carb}) (Li et al., 2012). These proxies are frequently used in the recognition of ancient oxic, anoxic, and euxinic environments (Poulton et al., 2004; Lyons and Gill, 2010). For example, the modern and ancient sediments have the empirically ratios that Fe_{HR}/Fe^T is less than 0.38 in oxic environments; and $Fe_{HR}/Fe^T > 0.38$ and $Fe_{py}/Fe_{HR} > 0.7$ indicate euxinic environments (Raiswell and Canfield, 1998; Poulton and Canfield, 2005).

Our results show that manganese ore layers, carbonaceous shale layers and silty shale layers have contrasting Fe chemistry (Table 1, Fig. 4). The lower portion of the section (samples D1-1~MN-2) have $Fe_{HR}/Fe^T > 0.38$ and $Fe_{py}/Fe_{HR} < 0.7$, indicative of ferruginous conditions. The upper portion of the section (samples D2~D15) show high Fe_{py}/Fe_{HR} ratios, generally more than 0.7 except that two shale samples ($Fe_{py}/Fe_{HR} = 0.68$), suggesting predominant euxinic environments (Table 1). The samples of the upper member (silty shales, samples D24~D26) have $Fe_{HR}/Fe^T < 0.38$, suggesting an oxic environment.

The $\delta^{34}S_{PY}$ of manganese ore ranges in 60.50‰~62.82‰, with average value of 61.66‰. The $\delta^{34}S_{PY}$ of carbonaceous shales and silty shales is 53.56‰~61.66‰, with an average of 57.8‰. Other studies have revealed that the sulfur isotope anomaly during the Cryogenian interglacial period is ubiquitous all over the world, generally in a range of 25‰~70‰ (Walter et al., 1995; Cui et al., 2018). The $\delta^{34}S_{PY}$ contents are

Table 3. Carbon and oxygen isotopic results.

Lithology	Carbonate shale		Silty shale		Manganese ore	
Samples	D2	D14	D5	D9	Mn-1	Mn-2
$\delta^{13}C$ (‰)	-7.90	-7.60	-7.26	-7.20	-7.64	-8.26
$\delta^{18}O$ (‰)	-12.20	-14.80	-15.26	-14.60	-9.25	-10.50

influenced by sulfate concentration and the biological function leading to sulfur isotope fractionation. The Nanhua Basin is of limited, closed basin so that the sulfate concentration in the deep water is low (Chen et al., 2008). When the sulfate concentration is relatively low, sulfur isotope fractionation by bacterial sulfate reduction process would become weak (Shen et al., 2003), and hence the $\delta^{34}S_{PY}$ values more possibly represent a heritage of original sulfur isotope constitution in deep water. More recently, Cui et al. (2018) revealed that the high $\delta^{34}S_{PY}$ values might be related to thermochemical sulfate reduction in hydrothermal fluids during late burial diagenesis. Although our data can't preclude this possibility of thermochemical sulfate reduction process, a reducing condition is suggested in the formation of pyrite and high $\delta^{34}S_{PY}$ fractionation. In contrast, D24-D26 layers of silty shale in the upper member might be an oxic environment due to extremely low pyrite content.

4.3 Carbon and oxygen isotopes

The analyzed C and O isotopes are listed in Table 3. The $\delta^{13}C$ shows negative values ranging from -8.26‰ to -7.2‰. The carbon contents are relevant to algae that can transfer carbon into organic materials, leading to the enrichment of $\delta^{13}C$ in waters. In contrast, degradation of organic matter would decrease the $\delta^{13}C$ value. The relatively negative $\delta^{13}C$ values suggest the carbonate minerals precipitation was accompanied with a predominant process of degradation of organic matter.

The $\delta^{18}O$ has values in a range between -15.26‰ and -9.25‰. It is generally accepted that $\delta^{18}O$ variation was influenced by temperature and diagenesis (Oktia et al., 1988; Nyame et al., 2006). In addition, dilution of fresh water can produce extremely negative $\delta^{18}O$ values (Fang, 2000). The negative $\delta^{18}O$ values in the Datangpo Formation might be related with great amounts of input of fresh water during the interglacial period.

5. Discussion

5.1 Paleoenvironment and organic matter accumulation

Our TOC and phosphorus data reveal that the carbonaceous shales bear very high organic matters. Modern studies revealed that microbial bloom is associated with water eutrophication (Wu et al., 2009), and volcanic ash brings nutrients into the water giving rise to water eutrophication and biological flouri-
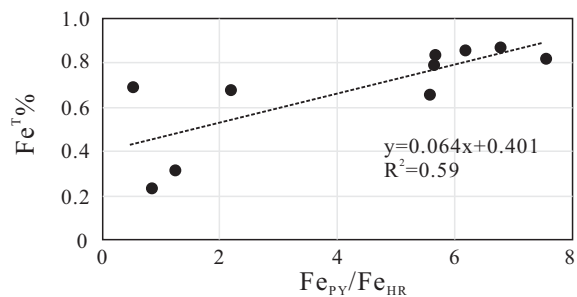
Fig. 5. Relationship between total iron and Fe_{py}/Fe_{HR} ratio.

shing. The negative $\delta^{18}O$ values in the Datangpo Formation imply that great amounts of input of fresh water during the interglacial period in the Nanhua Basin. Simultaneously, tuffaceous beds are frequently observed as lenses intercalated in the carbonaceous shale and the manganese ore beds (Yin et al., 2007; Zhou, 2013). The volcano eruptions along the breakup of Rodinian supercontinent were recorded as tuffaceous beds in the shales and it brought abundance nutrient substance that can lead to water eutrophication. Our study suggests that the organic matter is mainly amorphous I type kerogen, and the original organism is mainly algae (Fig. 2). The samples with high amount of phosphorus have more TOC, indicating that the biological flourishing is one of key factors to form abundant organic matters.

5.2 Redox condition and organic matter preservation

The redox state of ancient seawater is crucial to the preservation of organic matter. As the data mentioned above, the carbonaceous shales show $Fe_{HR}/Fe^T > 0.38$, Fe_{py}/Fe_{HR} is more than 0.7 indicating anoxic water environments. Moreover, the statistics of pyrite mineralization show that Fe_{py}/Fe_{HR} ratio and organic carbon content have a good positive correlation (Fig. 5). This reflects that the carbonaceous shale of the Datangpo Formation is formed in reducing and sulfidic environment. It is well known that organic matters will be limited to be degradation in anoxic condition. Therefore, the lower portion of the Datangpo Formation that is in a euxinic state is good for the preservation of organic matters. In contrast, the upper portion where deposited the silty shales and siltstones might be in an oxic environment due to low amount of pyrite and featured iron compositions. We consider that the upper portion deposited in an open system, fully exchange with overlying waters. The $\delta^{34}S_{PY}$ in the manganese ore and

$y=-0.815x+22.23$
$R^2=0.414$
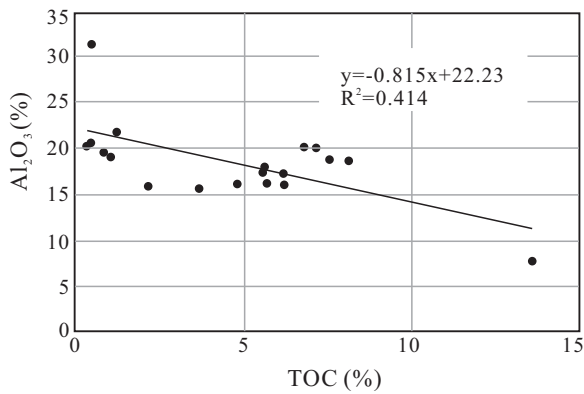
Fig. 6. Relationship between Al_2O_3 and TOC.

carbonaceous shales is higher than 50%. The sulfate reducing bacteria give priority to the reduction of S^{32} and continue to be supplemented. Therefore, the content of light sulfur isotopes increased significantly, while the heavy isotopes of sulfur decreased significantly. The light sulfur isotope is reduced first in the process of dissimilation reduction, and the S^{34} is enriched in the residual liquid. The enrichment degree is restricted by the contents of sulfate in pore water, active iron, organic matter and temperature (Dai et al., 2001; Huang et al., 2014). The fractionation of sulfur isotopes in the early stage of the Datangpo Formation is the result of active organic matter and sulfate biochemical action. Thus, the higher $\delta^{34}S_{PY}$ values imply a euxinic waters in deep portion and beneficial for the organic matter preservation. $\delta^{34}S_{PY}$ is reduced rapidly to 14.8‰-18.7‰ in the Datangpo Formation in shallow water environment, which indicated that the pore water can be fully exchanged with the overlying water (Li et al., 2012).

5.3 Terrestrial material input and organic matter dilution

High productivity is a necessary and sufficient condition for the enrichment of organic matter. But, the dilution effect of terrestrial source also has considerable influence on the content of organic carbon. The content of Al_2O_3 ranges from 7.7% to 31.6%, and the statistical results show a significant negative correlation between Al_2O_3 content and organic carbon content (Fig. 6). It is generally believed that Al_2O_3 is mainly derived from the weathered material in the continent, reflecting the degree of supply of terrigenous debris (Saito et al., 1992). Therefore, the intensive weathering and high inputs of terrestrial clasts will greatly dilute the organic carbonate contents.

6. Conclusions

This study shows iron compositions, sulfur isotope of pyrite, carbon and oxygen isotopes of the Datangpo Formation in the Datangpo section. These new data lead us to conclude that:

1) The carbonaceous shales that have high amount of phosphorus generally display more TOC. In addition, the

carbonaceous shales show relatively high oxygen isotopes, implying large volume of fresh water input in the Nanhua Basin during the interglacial gap. Considering the intercalated tuffaceous beds in the shales, we suggest that the biological flourishing during the interglacial period ensured sufficient supply of organic matters.

2) The euxinic environments provide ideal settings for the organic matter preservation. Our iron chemistry and sulfur isotope suggest the carbonaceous shales were in anoxic and euxinic deep waters. Although the $\delta^{34}C$ values are relatively negative, correlative to degradation of organic matter, the euxinic condition in deep waters ensures organic matter preservation. Terrestrial clasts might feed the shale sediments because some layers have high contents of Al_2O_3 and these terrestrial components greatly dilute the organic matters.

References

Arthur, M.A., Sageman, B.B. Marine black shales: Depositional mechanisms and environments of ancient deposits. Annu. Rev. Earth Planet. Sci. 1994, 22(1): 499-551.

Canfield, D.E., Raiswell, R., Westrich, J.T., et al. The use of chromium reduction in the analysis of reduced inorganic sulfur in sediments and shales. Chem. Geol. 1986, 54(1-2): 149-155.

Chen, X., Li, D., Ling, H., et al. Carbon and sulfur isotopic compositions of basal Datangpo Formation, northeastern Guizhou, South China: Implications for depositional environment. Prog. Nat. Sci. Mater. 2008, 18(4): 421-429.

Cohen, P.A., Knoll, A.H., Kodner, R.B. Large spinose microfossils in Ediacaran rocks as resting stages of early animals. Proc. Natl. Acad. Sci. USA 2009, 106(16): 6519-6524.

Cui, H., Kitajima, K., Spicuzza, M.J., et al. Questioning the biogenicity of Neoproterozoic superheavy pyrite by SIMS. Am. Mineral. 2018, 103: 1362-1400.

Dai, S., Ren, D., Tang, Y., et al. Model of surphur accumulation in the high-sulphur coal. Geological Review 2001, 47(4): 383-387. (in Chinese)

Dodd, M.S., Papineau, D., Grenne, T., et al. Evidence for early life in earth's oldest hydrothermal vent precipitates. Nature 2017, 543(7643): 60-64.

Fang, N. Application of carbon and oxygen isotopes in sequence stratigraphy, In Study on sequence stratigraphy

in China, edited by Wang, H.Z., Guangdong Science and Technology Press, Guangzhou, pp. 367-379, 2000. (in Chinese)

He, J., Ding, W., Jiang, Z., et al. Mineralogical and chemical distribution of the Es3^L Oil Shale in the Jiyang Depression, Bohai Bay Basin (E China): Implications for paleoenvironmental reconstruction and organic matter accumulation. Mar. Pet. Geol. 2017, 81: 196-219.

Huang, X., Ghu, M., Chen, L. Sources and formation mechanisms of organic sulfur in Jiaozhou Bay sediments. Acta Oceanologica Sinica 2014, 36(6): 50-57. (in Chinese)

Ilgen, A.G., Heath, J.E., Akkutlu, I.Y., et al. Shales at all Scales: Exploring coupled processes in mudrocks. Earth-Sci. Rev. 2017, 166: 132-152.

Jiang, S., Feng, Y., Chen, L., et al. Multiple-stacked hybrid plays of lacustrine source rock intervals: Case studies from lacustrine basins in China. Pet. Sci. 2017, 14(3): 459-483.

Johnson, R.C., Birdwell, J.E., Mercier, T.J., et al. Geology of tight oil and potential tight oil reservoirs in the lower part of the Green River Formation, Unita, Piceance, and Greater Green River Basin, Utah, Colorado, and Wyoming. In: U.S.G.S Scientific Investigations Report 2016, No. 2006-5005, 63.

Lazar, O.R., Bohacs, K.M., Macquaker, J.H.S., et al. Capturing key attributes of fine-grained sedimentary rocks in outcrops, cores, and thin sections: Nomenclature and description guidelines. J. Sediment. Res. 2015, 85(3): 230-246.

Li, C., Love, G.D., Lyons, T.W., et al. Evidence for a redox stratified Cryogenian marine basin, Datangpo Formation, South China. Earth Planet. Sci. Lett. 2012, 331: 246-256.

Li, C., Zhu, M., Chu, X. Preface: Atmospheric and oceanic oxygenation and evolution of early life on earth: New contributions from China. J. Earth Sci. 2016, 27(2): 167-169.

Liu, X., Jin, Z., Bai, G., et al. Formation and distribution characteristics of ProterozoicLower Paleozoic marine giant oil and gas fields worldwide. Pet. Sci. 2017, 14(2): 237-260.

Lyons, T.W., Gill, B.C. Ancient sulfur cycling and oxygenation of the early biosphere. Elements 2010, 6(2): 93-99.

Macdonald, F.A., Schmitz, M.D., Crowley, J.L., et al. Calibrating the Cryogenian. Science 2010, 327(5970): 1241-1243.

Nyame, F.K., Beukes, N.J. The genetic significance of carbon and oxygen isotopic variations in Mn-bearing carbonates from the Palaeo-Proterozoic ($\sim$2.2Ga) Nsuta Deposit in the Birimian of Ghana. Carbonates Evaporites 2006, 21(1): 21-32.

Okita, P.M., Maynard, J.B., Spiker, E.C., et al. Isotopic evidence for organic matter oxidation by manganese reduction in the formation of stratiform manganese carbonate ore. Geochim. Cosmochim. Acta 1988, 52(11): 2679-2685.

Planavsky, N.J., Rouxel, O.J., Bekker, A., et al. The evolution of the marine phosphate reservoir. Nature 2010,

467(7319): 1088-1090.

Poulton, S.W., Canfield, D.E. Development of a sequential extraction procedure for iron: Implications for iron partitioning in continentally derived particulates. Chem. Geol. 2005, 214(3-4): 209-221.

Poulton, S.W., Fralick, P.W., Canfield, D.E. The transition to a sulphidic ocean $\sim$1.84 billion years ago. Nature 2004, 431(7005): 173-177.

Raiswell, R., Canfield, D.E. Sources of iron for pyrite formation in marine sediments. Am. J. Sci. 1998, 298(3): 219-245.

Saito, C., Noriki, S., Tsunogai, S. Particulate Flux of A1, A component of land origin, in the Western North Pacific. Deep Sea Res. A 1992, 39(7-8): 1315-1327.

Scott, C., Lyons, T.W., Bekker, A., et al. Tracing the stepwise oxygenation of the Proterozoic ocean. Nature 2008, 452(7186): 456-459.

Shen, Y.N., Knoll, A.H., Walter, M.R. Evidence for low sulphate and anoxia in a Mid-Proterozoic marine basin. Nature 2003, 423(6940): 632-635.

Shi, G.Z., Song, G.Z., Wang, H., et al. Late Paleozoic tectonics of the Solonker Zone in the Wuliji area, Inner Mongolia, China: Insights from stratigraphic sequence, chronology, and sandstone geochemistry. J. Asian Earth Sci. 2016, 127: 100-118.

Shi, G., Song, G., Wang, H., et al. Provenance and tectonic setting of the Upper Palaeozoic sandstones in western Inner Mongolia (the Shalazhashan and Solonker belts), China: Insights from detrital zircon U-Pb ages and Hf isotopes. Geol. Mag. 2018, 1-25.

Walter, M., Veevers, J., Calver, C., et al. Neoproterozoic stratigraphy of the Centralian superbasin, Australia. Precambrian Res. 1995, 73(1-4): 173-195.

Wang, J. History of Neoproterozoic rift basins in South China: Implications for Rodinia break-up. Precambrian Res. 2003, 122(1-4): 141-158.

Wei, W., Wang, D., Li, D., et al. The marine redox change and nitrogen cycle in the Early Cryogenian interglacial time: Evidence from nitrogen isotopes and Mo contents of the basal Datangpo Formation, Northeastern Guizhou, South China. J. Earth Sci. 2016, 27(2): 233-241.

Wu, F., Wang, F., Wu, H., et al. Distributions of total phosphorus, phshorus fractions, and biogenic silica in dianchi lake and hongfeng lake sediments. Chinese Journal of Ecology 2009, 28(1): 88-94. (in Chinese)

Yeasmin, R., Chen, D., Fu, Y., et al. Climatic-oceanic forcing on the organic accumulation across the shelf during the Early Cambrian (Age 2 through 3) in the Mid-Upper Yangtze block, NE Guizhou, South China. J. Asian Earth Sci. 2017, 134: 365-386.

Yin, L., Zhu, M., Knoll, A.H., et al. Doushantuo embryos preserved inside diapause egg cysts. Nature 2007, 446(7136): 661-663.

Zhang, Q., Li, X., Feng, L., et al. A new age constraint on the onset of the Neoproterozoic Glaciations in the Yangtze Platform, South China. J. Geol. 2008, 116(4): 423-429.

Zhou, C., Tucker, R., Xiao, S., et al. New constraints on the ages of Neoproterozoic Glaciations in South China.

Geology 2004, 32(5): 437-440.

Zhou, Q., Du, Y., Qin, Y. Ancient natural gas seepage sedimentary-type manganese metallogenic system and ore-forming model: A case study of Datangpo type manganese deposits formed in rift basin of Nanhua Period along Guizhou-Hunan-Chongqing border area. Mineral Deposits 2013, 32(3): 457-466. (in Chinese)

Zhu, M., Strauss, H., Shields, G.A. From snowball Earth to the Cambrian bioradiation: Calibration of Ediacaran-Cambrian Earth history in South China. Palaeogeogr. Palaeocl. 2007, 254(1-2): 1-6.